IEEE Access
Multidisciplinary | Rapid Review | Open Access Journal

Received February 11, 2020, accepted March 8, 2020, date of publication March 12, 2020, date of current version March 20, 2020.

Digital Object Identifier 10.1109/ACCESS.2020.2980284

Wideband and Bandwidth-Controllable Hybrid-Cylindrical Glass Dielectric Resonator Antenna for Indoor Communication

XIAO SHENG FANG[1,2], (Member, IEEE), LING PENG WENG[1,2], AND YU XIANG SUN[3], (Member, IEEE)

[1]Department of Electronic and Information Engineering, Shantou University, Shantou 515063, China
[2]Guangdong Provincial Key Laboratory of Digital Signal and Image Processing, Shantou University, Shantou 515063, China
[3]College of Electronics and Information Engineering, Shenzhen University, Shenzhen 518060, China

Corresponding author: Xiao Sheng Fang (fangxs@stu.edu.cn)

This work was supported in part by the National Natural Science Foundation of China under Grant 61701292, in part by the Department of Education of Guangdong Province under Grant 2017KTSCX066, in part by the Shantou University Scientific Research Foundation for Talents under Grant NTF15008, and in part by the Natural Science Foundation of Shenzhen University under Grant 2019008.

ABSTRACT In this paper, a wideband and bandwidth-controllable hybrid-glass dielectric resonator antenna (DRA) excited by a probe platform is proposed. The proposed hybrid-glass DRA simply consists of a probe platform and a solid cylindrical glass DRA unit, making the fabrication easier. The probe mode and the $TM_{01\delta}$ mode of the cylindrical glass DRA are employed to design the wideband antenna. It is found that the impedance bandwidth of this hybrid-DRA can be controlled by the height of the glass DRA in a wide range of ∼23%-70%, without changing the size of the feeding. Engineering formula considering the bandwidth has been given to facilitate the design. To demonstrate the idea, three wideband hybrid-glass DRAs with their measured impedance bandwidths of 39.5%, 56.6% and 74% have been designed. To upgrade the three hybrid-glass DRAs as the artistic antennas, laser-engraving patterned glass is employed to do the fabrication again. The measured results show that the performance of the hybrid-glass DRAs with and without patterns are basically the same.

INDEX TERMS Hybrid-glass dielectric resonator antenna, wideband, bandwidth-controllable.

I. INTRODUCTION

Because of low loss and ease of excitation, the dielectric resonator antenna (DRA) [1]–[3] has been widely studied in the past three decades. Different kinds of materials can be used to fabricate a DRA, such as composite material, ceramics, and K9-glass. Among them the K9-glass is most interesting because of its transparent characteristics and beautiful appearance. In recent years, much work on the glass DRA has been reported, such as lens DRA [4], mirror DRA [5], socket DRA [6], light cover-DRA [7], [8] and artistic DRA [9], [10].

The radiation of DRA can be mainly divided into two types: directional and omnidirectional. For indoor communication, the omnidirectional DRA [11]–[13] is preferable to the directional one because it can cover a larger area. Generally, the impedance bandwidth of the fundamental TM mode of a solid DRA is less than 15% ($\varepsilon_r = 6.85$) [13].

The associate editor coordinating the review of this manuscript and approving it for publication was Jaime Laviada.

There are mainly two methods to widen the bandwidth of the omnidirectional DRA. The first method is to employ the higher-order modes. For instance, a cylindrical DRA loaded with an annular column was studied in [14]. This work successfully merges a fundamental and three higher-order TM modes of the cylindrical DRA, which provides an impedance bandwidth of 56 %. The second method is to apply the hybrid-DRA [15]–[23], which often combines the ring DRAs and the monopole antennas to achieve a wideband antenna. Unfortunately, both methods employ annular dielectric blocks inevitably, which are suitable for designing the DRA made of the composite material but not the glass. This is because glass is a typical brittle material that does not have ductility and plasticity at room temperature. It can not bear relatively large external forces or it will be crack easily. In other words, fabricating an annular glass is very difficult.

On the other hand, bandwidth-controllable antenna is more popular since it can help people to design the appropriate

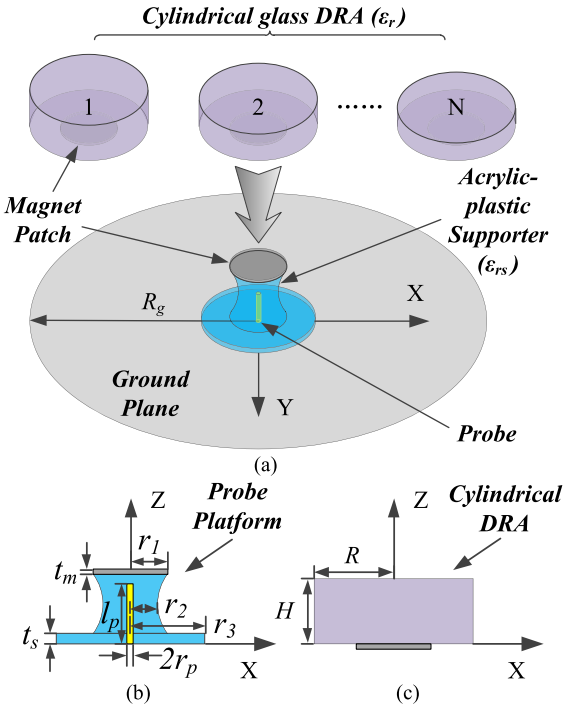

FIGURE 1. The configuration of the wideband and bandwidth-controllable hybrid-glass DRA. (a) The configuration of the proposed DRA. (b) The probe platform. (c) The cylindrical glass DRA unit.

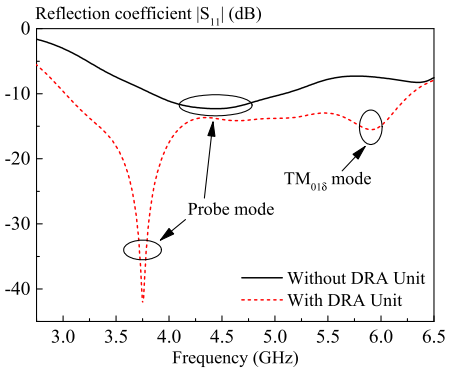

FIGURE 2. Simulated reflection coefficients of the proposed configuration with and without glass DRA unit: R_g = 100 mm, ε_r = 6.85, ε_{rs} = 2.5, r_1 = 7.5 mm, r_3 = 15 mm, t_s = 2 mm, t_m = 1 mm, l_p = 12 mm, R = 20 mm and H = 8 mm.

bandwidth according to their own needs. However, relatively little work on the bandwidth-controllable DRA has been reported. In [15], the bandwidth of a cylindrical ring DRA is controlled by using metal loading, in which the metal is used to suppress the radiation at high frequency band. But this method is also not suitable for designing the glass DRA, because the introduction of the metal on the top or outside surface of the DRA will destroy the transparency and aesthetics of the glass.

In this paper, a wideband and bandwidth-controllable hybrid-glass DRA for indoor communication is firstly proposed. The proposed DRA is made of a solid cylindrical

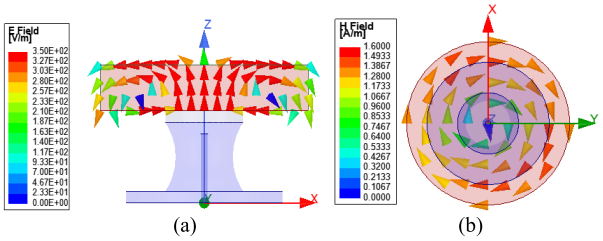

FIGURE 3. Simulated E/H-fields inside the glass DRA. (a) E-field of the $TM_{01\delta}$ mode at 5.92 GHz. (b) H-field of the $TM_{01\delta}$ mode at 5.92 GHz.

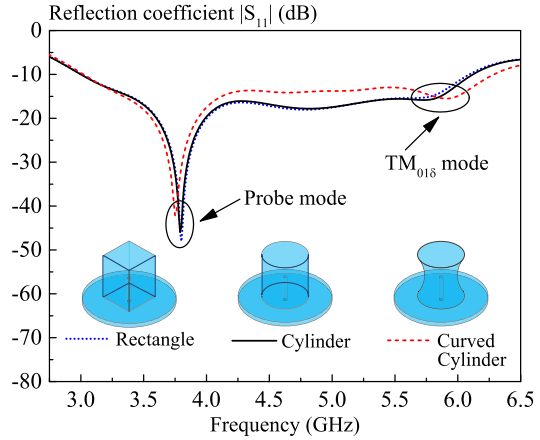

FIGURE 4. Simulated reflection coefficient of the proposed hybrid-DRA with acrylic-plastic supporter of different shapes: rectangle, cylinder and curved cylinder. The parameters are the same as in Fig. 2.

glass, which makes the fabrication easily. A probe platform is used to excite the DRA. By merging the probe and the $TM_{01\delta}$ mode of the cylindrical glass DRA, a wideband hybrid-DRA can be achieved. It is found that the impedance bandwidth of the antenna can be controlled by the height of the cylindrical glass in a wide frequency range. To facilitate the design, engineering formula considering the impedance bandwidth is derived using the covariance matrix adaptation evolutionary strategy (CMA-ES) [24], [25]. And three wideband hybrid-glass DRAs with impedance bandwidths of 39.5%, 56.6% and 74% were designed for the purpose of the demonstration. In addition, laser-engraving patterned glass is employed to update the hybrid-glass DRAs as the artistic antenna. It is found that the performance of the hybrid-glass DRAs with and without patterns are basically the same.

II. ANTENNA CONFIGURATION, RESONANT MODE AND BANDWIDTH

A. ANTENNA CONFIGURATION

The configuration of the proposed hybrid-glass DRA is shown in Fig. 1 (a). It consists of an aluminum groundplane of radius R_g = 100 mm, a probe platform and a solid cylindrical DRA unit made of K9-glass (ε_r = 6.85). In the section *D*, we will discuss that the impedance bandwidth of the antenna can be controlled by the height of the cylindrical

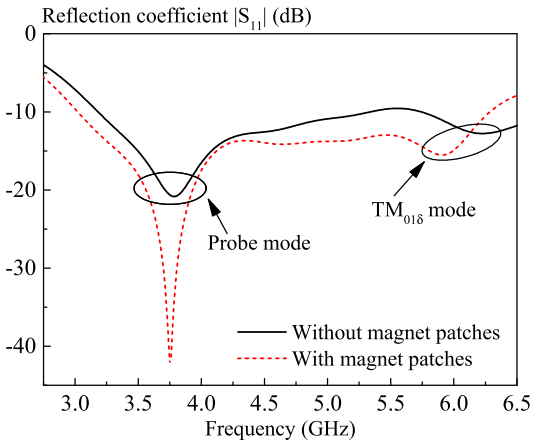

FIGURE 5. Simulated reflection coefficient of the proposed hybrid-DRA as a function of frequency: without and with magnet patches. The parameters are the same as in Fig. 2.

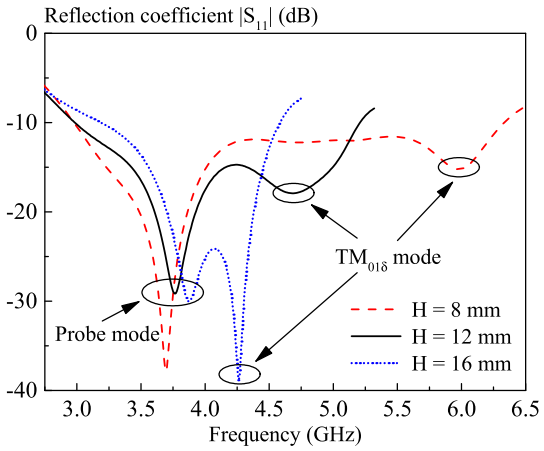

FIGURE 7. Simulated reflection coefficients of the proposed hybrid-glass DRA versus frequency: H = 8, 12, and 16 mm. Other parameters are the same as in Fig. 2.

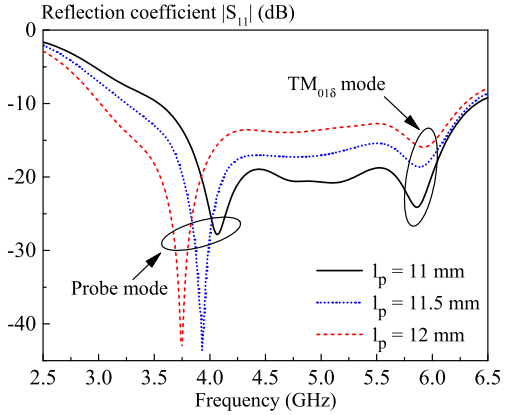

FIGURE 6. Simulated reflection coefficients of the proposed hybrid-glass DRA versus frequency: l_p = 11, 11.5, and 12 mm. Other parameters are the same as in Fig. 2.

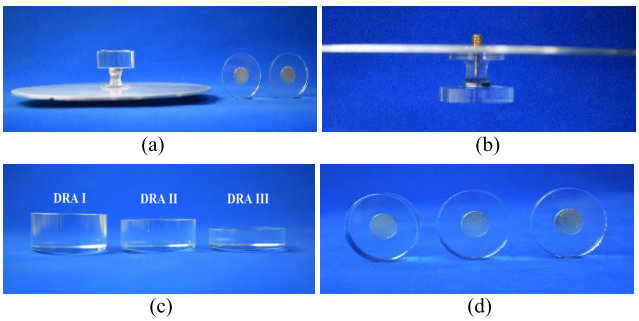

FIGURE 8. Prototype of the proposed hybrid-glass DRAs. (a) Overview of the hybrid-DRAs. (b) Upturned view of the hybrid-DRA. (c) Side view of the three glass DRAs. (d) Top face of the three glass DRAs.

glass. Therefore, N is used to represent the number of cylindrical glass DRAs of different heights. The probe platform unit is composed of a probe of length $l_p = 12$ mm and a curved-cylinder supporter made of transparent acrylic plastic ($\varepsilon_{rs} = 2.5$), as shown in Fig. 1 (b). The supporter is mainly composed of two parts: i) the upper part is a curved cylinder of radius $r_1 = 7.5$ mm; ii) the lower part is a flat disc of a radius $r_3 = 15$ mm and thickness $t_s = 2$ mm, which is used to fix with the groundplane. Each DRA unit has a radius of R and a height of H, as shown in Fig. 1(c). Two circular conducting magnet patches (NdFe30) with a thickness of $t_m = 1$ mm are centrally pasted at the bottom of the glass DRA and the top of the supporter, respectively. In this way, the DRA can be removed and replaced very easily.

B. RESONANT MODE

This part will investigate the resonant mode of the hybrid-glass DRA. To begin with, a solid cylindrical glass DRA of $R = 20$ mm and $H = 8$ mm was used in the simulation. Fig. 2 shows the simulated reflection coefficient without and with the glass DRA unit. With reference to the curve without the glass DRA unit, only one resonant mode observed at 4.27 GHz. This was due to the probe mode since its estimated resonance frequency $f_p = 3.96$ GHz ($f_p = c/4l_p\sqrt{\varepsilon_{rs}}$, where c denotes the velocity of light in vacuum) is close to the simulated one $f_s = 4.27$ GHz. With the glass DRA unit, the probe mode shifts downward and one more resonance mode was found around 5.9 GHz, which is due to the DRA mode. To further verify the DRA mode, the E-field and H-field around 5.9 GHz were studied in Fig. 3. With reference to the figure, its E-field is vertical and strongest along the z-axis whereas the H-field is circular around the z-axis in the region of the DR, showing it is the $TM_{01\delta}$ mode of the cylindrical glass DRA.

C. EFFECT OF THE ACRYLIC-PLASTIC SUPPORTER AND THE MAGNET PATCHES

In this part, the effects of the acrylic-plastic supporter and the magnet patches on the hybrid-glass DRA are studied. Fig. 4 shows the simulated reflection coefficient of the proposed hybrid-DRA with acrylic-plastic supporter of different shapes: rectangle, cylinder and curved cylinder. The heights and volumes of the three shapes are the same. As can be seen

TABLE 1. Summary of the designed, simulated and measured impedance bandwidths and application bands of the proposed hybrid-DRAs.

	Designed bandwidth	Simulated bandwidth	Measured bandwidth	Application bands	Measured gain range
DRA I	34%	35.8% (3.19-4.58GHz)	39.5% (3.17-4.73GHz)	5G band-n77	2.68-5.16dBi
DRA II	55%	55.1% (3.04-5.35GHz)	56.6% (2.99-5.35GHz)	5G band-n77, WLAN-5.2 GHz	1.97-4.29dBi
DRA III	70%	72% (2.98-6.33GHz)	74% (2.96-6.44GHz)	5G band-n77, WLAN-5.2/5.8GHz	1.99-5.1dBi

from the figure, the probe and the DRA modes merge together to form a wideband antenna. The results of the three case are basically the same, showing the shapes of the supporter have little effect on the hybrid-DRA. The curved cylinder is chosen in our final design since it is more aesthetic than the previous two. It is worth mentioning that acrylic is not easy to be damaged under external force. Hence, it is allowed to make different shapes or drill hole for accommodating the probe. In other words, fabricating the acrylic part is not difficult. Fig. 5 shows the simulated reflection coefficient of the proposed hybrid-DRA without and with magnet patches. With reference to the figure, the magnet patches can improve the matching of the antenna obviously. This is reasonable because the diameter of the magnet is larger than that of the probe, indicating more energy can be transferred to the glass DRA by the magnet patches.

D. ANALYSIS OF THE BANDWIDTH CONTROL

In this part, the impedance bandwidth of the hybrid-glass DRA is investigated. Fig. 6 shows the simulated reflection coefficient of the hybrid-glass DRA as a function of frequency for different l_p = 11 mm, 11.5 mm, 12 mm. As can been see from the figure, the impedance bandwidth of the proposed antenna can be controlled by the length of the probe l_p, but with a relatively narrow controlled bandwidth range of ∼58%-70% obtained. Fig. 7 shows the simulated reflection coefficient of the hybrid-glass DRA as a function of frequency for different H = 8 mm, 12 mm and 16 mm. As can be seen from the figure, the impedance bandwidth can be also controlled by the height of the glass DRA independently. And the controlled bandwidth range can be achieved as ∼23%-70%, which is much wider than that of using the probe length as mention earlier. Therefore, the height of the glass DRA is chosen to control the bandwidth in this article. The effect of the radius of the DRA on the reflection coefficient has also been studied, it was found that the radius is not very sensitive to the impedance bandwidth of the antenna. For simplicity, the result is not shown here.

As studied above, the impedance bandwidth of the hybrid-DRA is inversely proportional to H when l_p and R are set. To facilitate the design, a number of data sets were generated using the HFSS, and the CMA-ES method [24], [25] was employed to obtain the following formula:

$$t = -5.059B^3 + 7.765B^2 - 4.918B + 1.772 \qquad (1)$$

where $t = H/R$, and B denotes the simulated impedance bandwidth of the hybrid- glass DRA. The formula is valid in the range of 22.7 % ≤ B ≤ 70.2 %, with $l_p/R = 0.6$.

E. DESIGN GUIDELINE

The design guideline of the wideband and bandwidth-controllable hybrid-glass DRA is summarized as follows:

i) Set the required impedance bandwidth B and f_L,in which f_L denotes the minimum frequency of the antenna in the working frequency band.
ii) Calculate the length of the probe: $l_p = c/(4f_p\sqrt{\varepsilon_{rs}})$, where $f_p \sim 1.28\,f_L$.
iii) Calculate the radius of the glass DRA: $R \sim 1.67l_p$.
iv) Calculate the height of the glass DRA using formula (1).

III. DESIGN EXAMPLE

In this part, design example of the wideband and bandwidth-controllable hybrid-glass DRAs is given. We take the coverage of band-n77 for the China-5G communication (3.3-4.2 GHz) as the design goal. Hence, f_L is arbitrarily chosen as 3.08 GHz, which is nearby the application band. The number of the glass DRA units are chosen as N = 3 and their impedance bandwidths are chosen as 34 %, 55 % and 70 %, respectively. Following the design guideline (ii) and (iii), l_p = 12 mm and R = 20 mm are obtained. The height of the DRA I, DRA II and DRA III can be obtained as H = 16 mm, 11.5 mm and 8 mm using the formula (1), respectively. The prototype of the proposed hybrid-glass DRAs are shown in Fig. 8. As can be seen from the Fig. 8 (b), the DRA is firmly connected to the groundplane by the magnet patch and will not fall down even if it is placed upside down.

Fig. 9(a)-(c) shows the simulated and measured reflection coefficient of the three hybrid-glass DRAs, respectively. With reference to the figure, reasonable agreement between the simulation and the measurement is obtained. The measured impedance bandwidth of the DRA I, DRA II and DRA III can be achieved as 39.5% (3.17-4.73GHz), 56.6% (2.99-5.35GHz) and 74% (2.96-6.44GHz), respectively. Table 1 summaries the designed, simulated and measured impedance bandwidths of the DRAs and their application bands. As can be seen from the table, the designed, simulated and measured bandwidths are basically consistent, verifying the validity of the formula. In addition, the application frequency bands covered by the proposed hybrid-glass DRAs are optional. The antenna gains

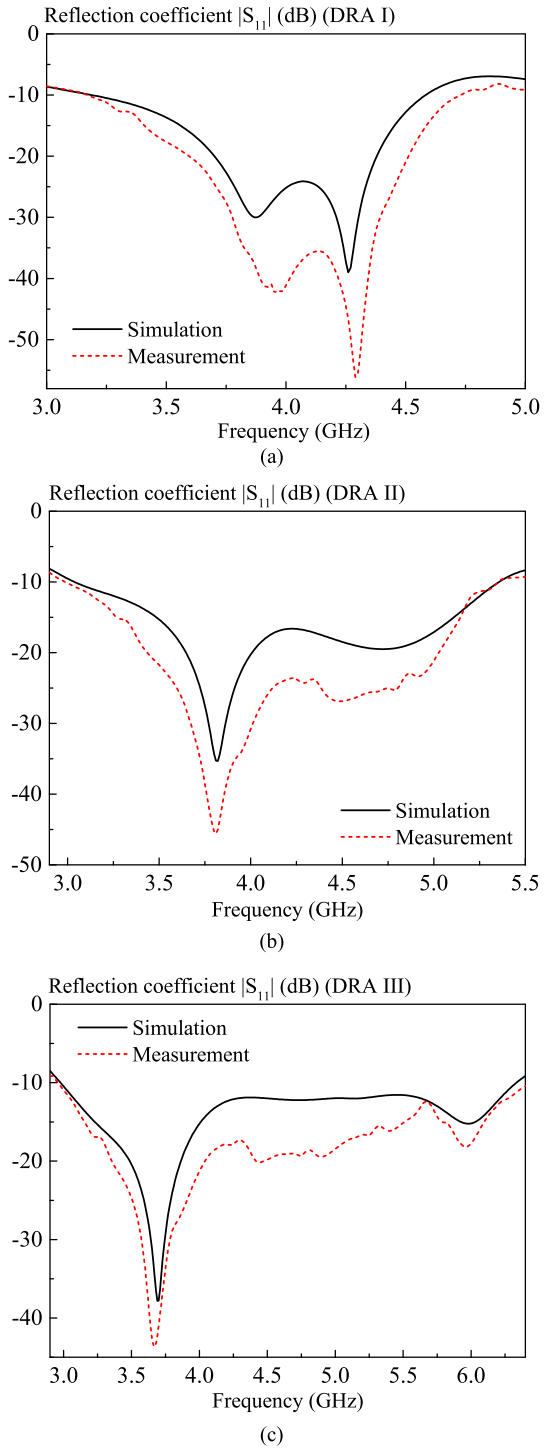

FIGURE 9. Simulated and measured antenna reflection coefficients of the proposed DRAs versus frequency: (a) DRA I. (b) DRA II. (c) DRA III.

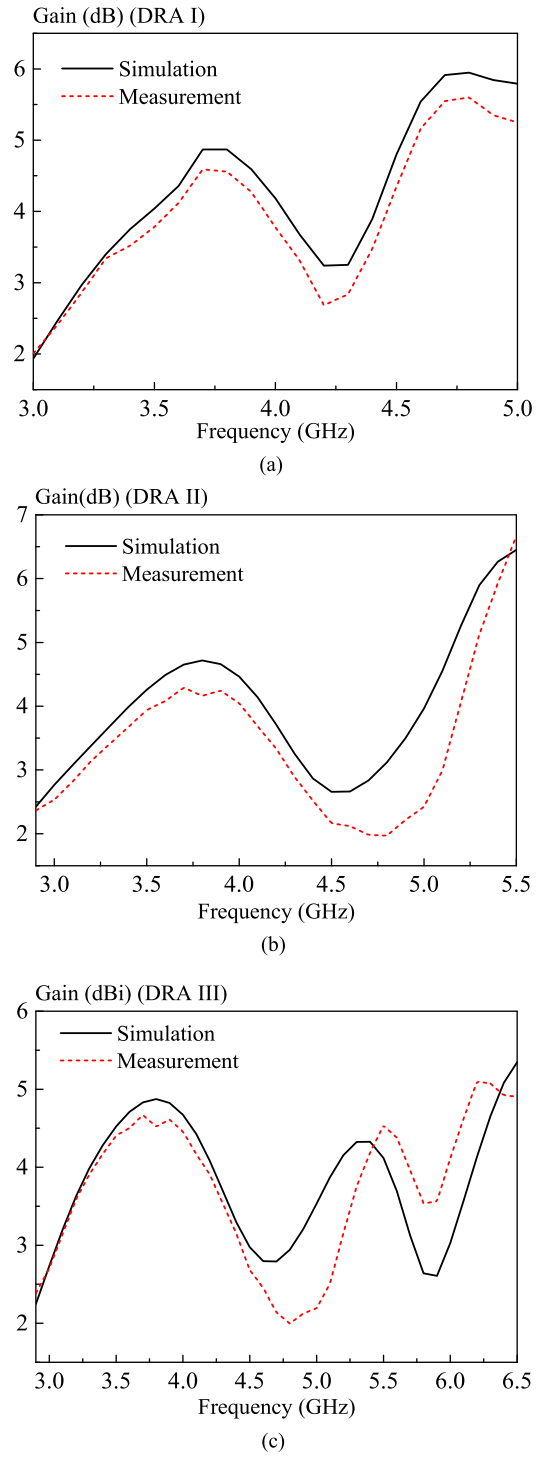

FIGURE 10. Simulated and measured antenna gains of the proposed DRAs versus frequency: (a) DRA I. (b) DRA II. (c) DRA III.

($\theta = 45°$, $\Phi = 0°$) of the three hybrid-glass DRAs are shown in Fig. 10(a)-(c), respectively. As can be seen from the figure, the minimum gain of the hybrid-DRAs is over than 0 dBi, showing they are the qualified antennas. The gain range of the three hybrid-glass DRA are also summarized in Table 1.

The radiation patterns of the three hybrid-glass DRAs were also studied. Fig. 11 shows the simulated and measured radiation patterns of the DRA III at 3.5 GHz and 5.85 GHz, respectively. With reference to the figure, omnidirectional radiation pattern was observed, as expected. The radiation

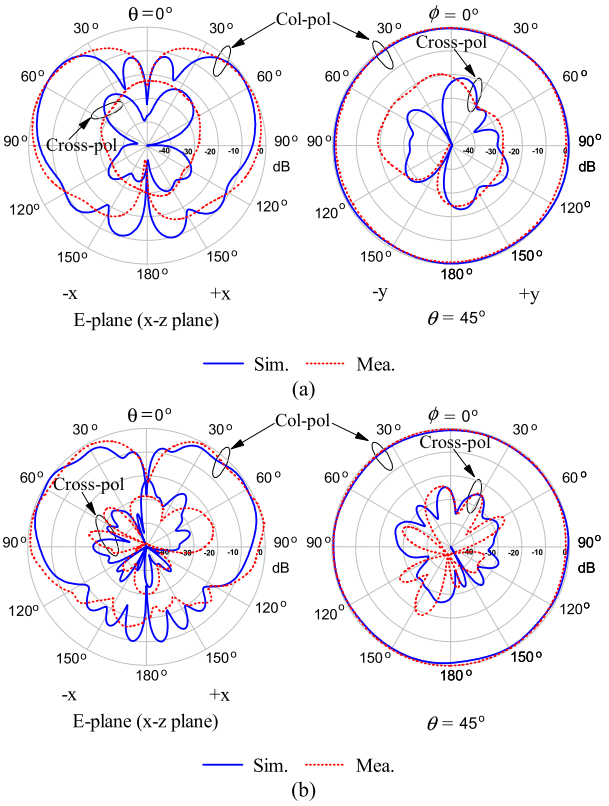

FIGURE 11. Simulated and Measured radiation patterns of the hybrid-DRA III. (a) Probe mode at 3.5 GHz. (b) DRA mode at 5.85 GHz.

TABLE 2. Comparison of different wideband solid DRAs with omnidirectional radiation patterns.

Reference	DRA type	ε_r	Impedance Bandwidth	Bandwidth-controllable
[11]	Solid	36.6	8%	No mention
[12]	Solid	10	19%	No mention
[13]	Solid	6.85	14%	No mention
[14]	Solid+ring	9	56%	No mention
Proposed	Solid	6.85	74% (Max.)	Yes

patterns of the DRA I and DRA II are similar to that in Fig. 11. For simplicity, the result is not shown here.

Table 2 compares our hybrid-glass DRA with other solid omnidirectional DRAs. With reference to the table, the maximum impedance bandwidth of the proposed hybrid-DRA is obviously larger than those designed by the solid DRA [11]–[13], and competitive with the solid + ring structure in [14]. Also, only our hybrid-glass DRA is mentioned to be bandwidth-controllable.

To further upgrade the glass DRA as the artistic antenna, patterns of ''Cat'', ''Flower'' and ''Santa Claus'' were engraved inside the DRA I, DRA II and DRA III by using the laser, respectively. Their prototypes are shown in Fig.12. Fig. 13 shows the measured reflection coefficients of the three hybrid-DRAs with patterns. For ease of comparison, the measured results without patterns are also shown in the

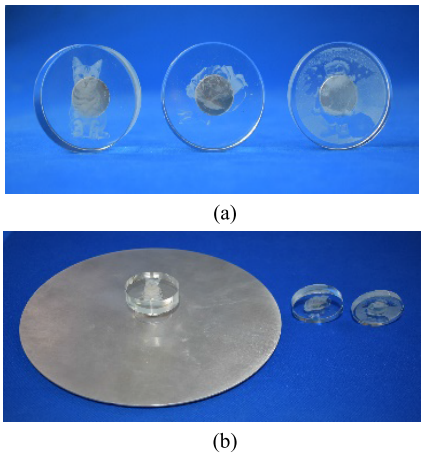

FIGURE 12. Prototype of the proposed hybrid-glass DRAs with patterns. (a) Top face of the three DRAs. (b) Overview of the hybrid-DRAs.

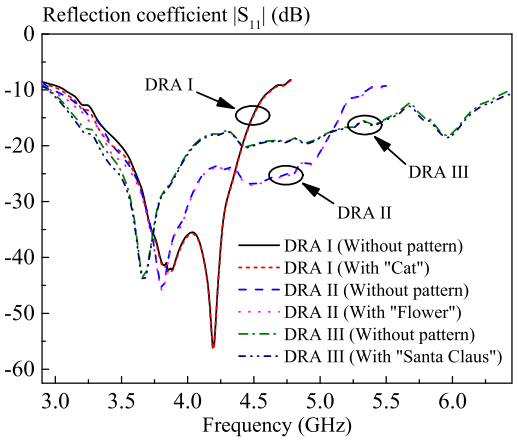

FIGURE 13. Measured reflection coefficients of the proposed three hybrid-DRAs without and with patterns.

same figure. As can be seen from the figure, the results with and without patterns are basically the same. This is expected because the feature size of the laser-engraving patterns is substantially smaller than the wavelength of the antenna.

IV. CONCLUSION

A wideband and bandwidth-controllable hybrid-glass DRA has been firstly investigated. The antenna configuration simply consists of a probe platform and a solid cylindrical glass DRA unit. Comparing to other wideband ring DRAs, the proposed hybrid-glass DRA is easier to fabricate. Two magnet patches for improving the antenna matching have been applied to fix the two units. In this way, the glass DRA can be removed and replaced easily. It has been found that the impedance bandwidth of this hybrid-DRA can be controlled by the height of the glass DRA in a wide frequency range, without changing the size of the feeding. Design formula and guideline have been given to facilitate the design. To demonstrate the idea, three wideband hybrid-glass DRAs with impedance bandwidths of 39.5%, 56.6%

and 74% have been designed. Therefore, users can choose the DRAs with appropriate impedance bandwidth at will. Moreover, laser-engraving patterned glass has been used to fabricate the hybrid-glass DRAs as the artistic antennas. It has been found that the performance of the hybrid-glass DRAs with and without patterns are basically the same. It should be mentioned that the proposed hybrid-glass DRA structure can also be applied to other DRAs made of composite material.

REFERENCES

[1] S. Long, M. McAllister, and L. Shen, "The resonant cylindrical dielectric cavity antenna," *IEEE Trans. Antennas Propag.*, vol. 31-AP, no. 3, pp. 406–412, May 1983.
[2] K. M. Luk and K. W. Leung, *Dielectric Resonator Antennas*. Oxford, U.K.: Research Studies Press, 2003.
[3] A. Petosa, *Dielectric Resonator Antenna Handbook*. Norwood, MA, USA: Artech House, 2007.
[4] E. H. Lim and K. W. Leung, "Transparent dielectric resonator antennas for optical applications," *IEEE Trans. Antennas Propag.*, vol. 58, no. 4, pp. 1054–1059, Apr. 2010.
[5] N. Yang, K. W. Leung, and E. H. Lim, "Mirror-integrated dielectric resonator antenna," *IEEE Trans. Antennas Propag.*, vol. 62, no. 1, pp. 27–32, Jan. 2014.
[6] L. Guo, K. W. Leung, S. Q. Wang, and K. F. Tsang, "Investigation of antenna-integrated transparent socket panel," *IEEE Access*, vol. 6, pp. 73001–73008, 2018.
[7] K. W. Leung, Y. M. Pan, X. S. Fang, E. H. Lim, K.-M. Luk, and H. P. Chan, "Dual-function radiating glass for antennas and light Covers—Part I: Omnidirectional glass dielectric resonator antennas," *IEEE Trans. Antennas Propag.*, vol. 61, no. 2, pp. 578–586, Feb. 2013.
[8] K. W. Leung, X. S. Fang, Y. M. Pan, E. H. Lim, K. M. Luk, and H. P. Chan, "Dual-function radiating glass for antennas and light Covers—Part II: Dual-band glass dielectric resonator antennas," *IEEE Trans. Antennas Propag.*, vol. 61, no. 2, pp. 587–597, Feb. 2013.
[9] K. W. Leung, E. H. Lim, and X. S. Fang, "Dielectric resonator antennas: From the basic to the aesthetic," *Proc. IEEE*, vol. 100, no. 7, pp. 2181–2193, Jul. 2012.
[10] X. S. Fang and S. M. Chen, "Design of the wide dual-band rectangular souvenir dielectric resonator antenna," *IEEE Access*, vol. 7, pp. 161621–161629, 2019.
[11] L. K. Hady, D. Kajfez, and A. A. Kishk, "Triple mode use of a single dielectric resonator," *IEEE Trans. Antennas Propag.*, vol. 57, no. 5, pp. 1328–1335, May 2009.
[12] L. Zou, D. Abbott, and C. Fumeaux, "Omnidirectional cylindrical dielectric resonator antenna with dual polarization," *IEEE Antennas Wireless Propag. Lett.*, vol. 11, pp. 515–518, 2012.
[13] X. S. Fang and K. W. Leung, "Design of wideband omnidirectional two-layer transparent hemispherical dielectric resonator antenna," *IEEE Trans. Antennas Propag.*, vol. 62, no. 10, pp. 5353–5357, Oct. 2014.
[14] Y. He, Y. Lin, C. Deng, and Z. Feng, "Annular column loaded cylindrical dielectric resonator antenna for wideband conical radiation," *IEEE Trans. Antennas Propag.*, vol. 63, no. 12, pp. 5874–5878, Dec. 2015.
[15] L. A. Shaik, C. Saha, S. Arora, S. Das, J. Y. Siddiqui, and A. K. Iyer, "Bandwidth control of cylindrical ring dielectric resonator antennas using metallic cap and sleeve loading," *IET Microw., Antennas Propag.*, vol. 11, no. 12, pp. 1742–1747, Sep. 2017.
[16] Y.-X. Guo, Y.-F. Ruan, and X.-Q. Shi, "Wide-band stacked double annular-ring dielectric resonator antenna at the end-fire mode operation," *IEEE Trans. Antennas Propag.*, vol. 53, no. 10, pp. 3394–3397, Oct. 2005.
[17] M. N. Jazi and T. A. Denidni, "Design and implementation of an ultrawideband hybrid skirt monopole dielectric resonator antenna," *IEEE Antennas Wireless Propag. Lett.*, vol. 7, pp. 493–496, 2008.
[18] M. Lapierre, Y. M. M. Antar, A. Ittipiboon, and A. Petosa, "Ultra wideband monopole/dielectric resonator antenna," *IEEE Microw. Wireless Compon. Lett.*, vol. 15, no. 1, pp. 7–9, Jan. 2005.
[19] D. Guha, B. Gupta, and Y. M. M. Antar, "Hybrid monopole-DRAs using Hemispherical/ conical-shaped dielectric ring resonators: Improved ultrawideband designs," *IEEE Trans. Antennas Propag.*, vol. 60, no. 1, pp. 393–398, Jan. 2012.
[20] C. Ozzaim, F. Ustuner, and N. Tarim, "Stacked conical ring dielectric resonator antenna excited by a monopole for improved ultrawide bandwidth," *IEEE Trans. Antennas Propag.*, vol. 61, no. 3, pp. 1435–1438, Mar. 2013.
[21] C. Ozzaim, "Monopole antenna loaded by stacked annular ring dielectric resonators for ultrawide bandwidth," *Microw. Opt. Technol. Lett.*, vol. 56, no. 10, pp. 2395–2398, Oct. 2014.
[22] D. Guha, Y. M. M. Antar, A. Ittipiboon, A. Petosa, and D. Lee, "Improved design guidelines for the ultra wideband monopole-dielectric resonator antenna," *IEEE Antennas Wireless Propag. Lett.*, vol. 5, pp. 373–376, 2006.
[23] D. Guha, B. Gupta, and Y. M. M. Antar, "New pawn-shaped dielectric ring resonator loaded hybrid monopole antenna for improved ultrawide bandwidth," *IEEE Antennas Wireless Propag. Lett.*, vol. 8, pp. 1178–1181, 2009.
[24] N. Hansen, S. D. Müller, and P. Koumoutsakos, "Reducing the time complexity of the derandomized evolution strategy with covariance matrix adaptation (CMA-ES)," *Evol. Comput.*, vol. 11, no. 1, pp. 1–18, Mar. 2003.
[25] M. D. Gregory, Z. Bayraktar, and D. H. Werner, "Fast optimization of electromagnetic design problems using the covariance matrix adaptation evolutionary strategy," *IEEE Trans. Antennas Propag.*, vol. 59, no. 4, pp. 1275–1285, Apr. 2011.

XIAO SHENG FANG (Member, IEEE) received the B.Eng. degree in electronic engineering from Sun Yat-Sen University, Guangzhou, China, in 2008, and the Ph.D. degree in electronic engineering from the City University of Hong Kong, Hong Kong, in 2012. From 2012 to 2015, he was a Senior Research Assistant with the Department of Electronic Engineering, City University of Hong Kong. He is currently an Associate Professor with the Department of Electronic Engineering, Shantou University, Shantou, China. His research interests include microwave antennas, dielectric resonator antennas, and passive RF components.

LING PENG WENG was born in Fuzhou, Fujian, China, in 1995. He received the B.E. degree in electronics and information engineering from Huaqiao University, in 2017. He is currently pursuing the master's degree in engineering with Shantou University. His research interests include dielectric resonator antennas, microwave antennas, and wireless communication.

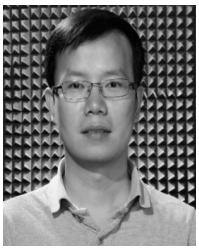

YU XIANG SUN (Member, IEEE) was born in Yingcheng, Hubei, China, in November 1987. He received the B.Eng. degree in electronic information science and technology and the M.Sc. degree in radio physics from Wuhan University, Wuhan, China, in 2010 and 2012, respectively, and the Ph.D. degree in electronic engineering from the City University of Hong Kong, in 2016.

From August 2012 to July 2013 and from October 2016 to February 2019, he was a Research Assistant and a Postdoctoral Fellow with the City University of Hong Kong. He joined the College of Electronics and Information Engineering, Shenzhen University, as an Assistant Professor, in March 2019. His current research interests include dielectric resonator antennas (DRA), millimeter-wave antennas, and circularly-polarized antennas.

He currently serves as a Technical Reviewer for the IEEE TRANSACTIONS ON ANTENNAS AND PROPAGATION, the IEEE ANTENNAS AND WIRELESS PROPAGATION LETTERS, and *IET Microwaves, Antennas and Propagation*.